

A Weak Donor, Planar Chelating Bitriazole N-Heterocyclic Carbene Ligand for Ruthenium(II), Palladium(II), and Rhodium

Macarena Poyatos,[†] William McNamara,[†] Chris Incarvito,[†] Eric Clot,[‡] Eduardo Peris,^{*,§} and Robert H. Crabtree^{*,†}

Chemistry Department, Yale University, 225 Prospect Street, New Haven, Connecticut 06511, Institut Charles Gerhardt Montpellier, UMR 5253 CNRS-UM2-ENSCM-UM1, Case Courrier 1501, Place Eugène Bataillon, 34095 Montpellier Cedex 5, France, and Departamento de Química Inorgánica y Orgánica, Universitat Jaume I, Avenida Vicente Sos Baynat s/n, Castellón E-12071, Spain

Received January 9, 2008

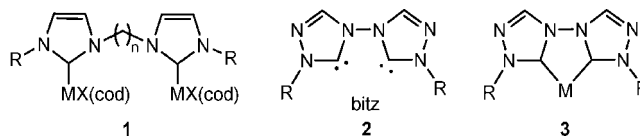
The new ligand bitriazole-2-ylidene (bitz) has been successfully coordinated to Ru(II), Pd(II), Rh(I), Rh(II), and Rh(III), showing its wide chemical versatility. Reaction of the bitz ligand precursor salt, 1,1'-methyl-4,4'-bi-1,2,4-triazolium diiodide, with [RhCl(cod)]₂ under mild conditions afforded chelate and bis-chelate Rh(III) complexes, as well as an unexpected metal–metal bounded di-Rh(II) species. The reaction of the precursor salt of bitz with [(η⁶-p-cymene)RuCl₂]₂ and NaOAc afforded a mixture of chelate and dimetallic Ru(II)-arene complexes. The reaction of the salt with Pd(OAc)₂ led to a chelate complex. In an unexpected, purely organic reaction, the precursor salt rearranges to a new C–C bound bitriazole on reaction with strong base in the absence of the metal. The electron-donor power of the bitz ligand, estimated by DFT computations, proved to be very low for an NHC and comparable with those of dmpe and dipy. Some of the new complexes proved to be catalytically active in hydrogen transfer from ¹PrOH.

Introduction

N-Heterocyclic carbenes (NHCs) have emerged as an extremely useful class of ligands for both transition metal-based catalysis^{1,2} and organocatalysis.³ Critical to any ligand set are steric and electronic tuning and accessibility of chelate forms. While these points are well established in phosphine chemistry, they are far from being fully worked out for NHCs. Change of the N-substituents has a large effect on the overall steric bulk but has a limited influence on electronic effect, tuning of which is more effectively managed by change of the azole ring, as for example by moving to C4(5)-bound NHCs to enhance donor power⁴ or to triazole-based NHCs to minimize donor power.⁵ In this paper we show that the electronic effect of a bitriazole-based NHC is very much decreased relative to the nonchelate form by inter-ring electronic effects, not present in seemingly analogous systems such as 2,2'-dipyridyl.

Chelating bis-NHCs in general are of great interest since they greatly extend the range of possible NHC ligands and allow delicate tuning of topological properties such as steric hindrance, bite angle, chirality, and fluxional behavior.^{6,7} Unfortunately,

Chart 1. Comparison of Related Bidentate N-Heterocyclic Ligands. From Left to Right: Nonchelating Binuclear Species (1), bitz Ligand (2), and Chelate Metal Complex Bearing bitz Ligand (3)



the linkers typically used for NHCs sometimes promote the formation of undesired nonchelating binuclear species such as **1** (Chart 1). In addition, the (CH₂)_n (n ≥ 2) linkers typically used are potentially subject to degradation via the Hoffmann elimination pathway in the presence of strong bases. Improved chelating bis-NHC ligands are therefore desirable. In this paper, we report on 1,1'-dimethyl-4,4'-bi-1,2,4-triazol-5,5'-ylidene (bitz, **2**), one of the simplest possible chelating bis-NHC ligands.

NHC ligands are normally among the strongest neutral donors. In contrast, bitz proves to lie at the low extreme of donor power among NHCs and is comparable in this respect with the very useful classical ligands 2,2'-dipyridyl and bis(dimethylphosphino)ethane. In contrast with the bent conformation of typical chelating NHCs, bitz is also flat, like 2,2'-dipyridyl.

A potential advantage of **2** could be a higher tendency to give the chelating structure **3** rather than the bridging structure **1**, since a highly favored five-membered chelate ring is formed upon coordination. The triazol-2-ylidene unit was chosen because the parent triazole is readily available⁸ and the electron-donor power of the ligand is expected to be lower than that of the corresponding imidazol-2-ylidene analogues and potentially similar to the range seen for the very successful phosphine ligand set.⁹ We now report on the electron-donor parameter of **2** and its organometallic chemistry with rhodium, ruthenium, and palladium, showing its wide chemical versatility. Our prelimi-

* To whom correspondence should be addressed. E-mail: robert.crabtree@yale.edu; eperis@qio.uji.es.

[†] Yale University.

[‡] Université Montpellier 2.

[§] Universitat Jaume I.

(1) Herrmann, W. A. *Angew. Chem., Int. Ed.* **2002**, *41*, 1291.

(2) Peris, E.; Crabtree, R. H. *Coord. Chem. Rev.* **2004**, *248*, 2239.

(3) Marion, N.; Diez-Gonzalez, S.; Nolan, S. P. *Angew. Chem., Int. Ed.* **2007**, *46*, 2988.

(4) Chianese, A. R.; Kovacevic, A.; Zeglis, B. M.; Faller, J. W.; Crabtree, R. H. *Organometallics* **2004**, *23*, 2461.

(5) Perrin, L.; Clot, E.; Einselestein, O.; Loch, J.; Crabtree, R. H. *Inorg. Chem.* **2001**, *40*, 5806.

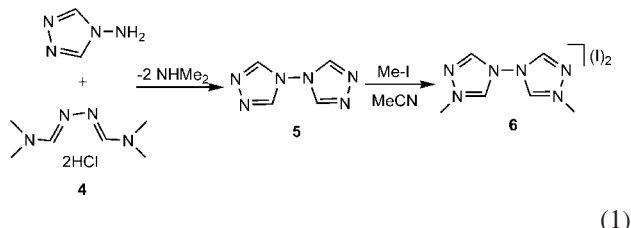
(6) Mata, J. A.; Poyatos, M.; Peris, E. *Coord. Chem. Rev.* **2007**, *251*, 841.

(7) Peris, E.; Crabtree, R. H. *C. R. Chim.* **2003**, *6*, 33.

nary results on the coordination of bitz ligand to rhodium have recently appeared in a communication.¹⁰

Results and Discussion

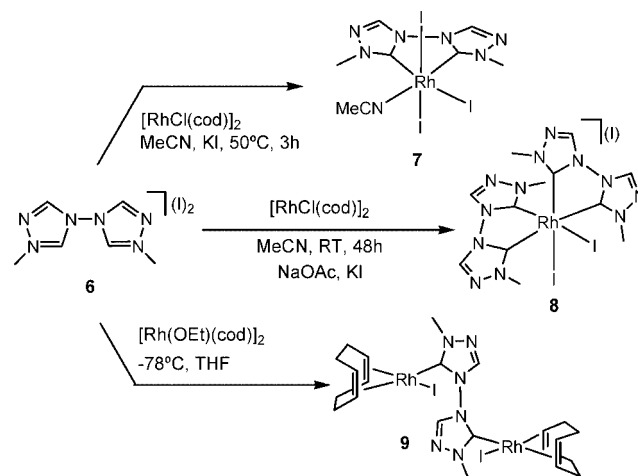
Synthesis of the Ligand Precursor and Its Coordination to Rhodium. The synthesis of 4,4'-bi-1,2,4-triazole (**5**) was carried out from *N,N*-dimethylformamide azine dihydrochloride (**4**) and 4-amino-1,2,4-triazole (eq 1), as previously reported by Bartlett and Humphrey.⁸ The bitz ligand precursor salt **6** was isolated in high yield upon N-quaternization of each triazole ring with MeI.¹¹



The reaction of precursor salt **6** with $[\text{RhCl}(\text{cod})]_2$ in MeCN at 50 °C, in the presence of KI, afforded the chelating monobitz complex **7** (Scheme 1). Remarkably, in contrast with previous cases, the addition of an external base was not needed to achieve the metalation. The coordination of the bitz ligand therefore occurs under milder conditions than usually found for other NHC precursor salts, which typically require prior base activation. The protons in the 5 position of bitz salt precursor **6** are expected to be much more acidic than those of typical NHC precursor salts because the triazole ring system is expected to be more electron withdrawing than imidazole and because the two azole rings are directly linked, so each acts as an electron-withdrawing substituent for the other.

The coordination sphere about the rhodium atom in **7** is completed by one MeCN and three iodo ligands. The NMR spectroscopic data are consistent with the proposed structure, the ligand C_2 symmetry being lost upon coordination. In particular, the ^{13}C NMR spectrum shows two doublets for the distinct carbene carbons at δ 166.5 ($^1J_{\text{Rh}-\text{C}} = 42.4$ Hz) and 158.2 ($^1J_{\text{Rh}-\text{C}} = 43.8$ Hz). As depicted in Scheme 1, when the reaction was carried out in the presence of the mild base NaOAc, the chelating bis-bitz complex **8** was isolated. This bis-chelate species is formed even with a 1:1 ratio of Rh:bitz, but a 1:2 ratio is preferred for higher yield. As expected for this structure, two inequivalent carbene atoms [δ 167.1 ($^1J_{\text{Rh}-\text{C}} = 34.9$ Hz) and 162.7 ($^1J_{\text{Rh}-\text{C}} = 43.6$ Hz)] and two signals due to the N-methyl groups (at 42.3 and 38.9 ppm, respectively) were observed in the ^{13}C NMR spectrum of **8**. One question that remains unanswered is how the oxidation from Rh(I) to Rh(III) occurs in the formation of the bis-carbene Rh(III) complexes **7** and **8**. One possible explanation is that traces of oxygen may oxidize I^- to I_2 , which in turn oxidatively adds to the Rh(I) complex, as previously suggested for related Rh(III) bis-NHC complexes.¹² However, the synthesis was carried out with strict exclusion of air. Another possibility is that the coordination of bitz goes by an oxidative addition of the bitriazolium salt C5–H

Scheme 1. Synthesis of Chelate and Bis-chelate Rh(III) Complexes **7** and **8** and of the Binuclear Rh(I) Complex **9**



bond, followed by σ -bond metathesis between the second C5–H bond and the rhodium hydride, with subsequent release of H_2 , as we found in previous cases.¹³

In our efforts to isolate the chelate-Rh(I) species, we followed the procedure employed by Cesar et al.¹⁴ for the coordination of carbene-oxazoline ligands to Rh(I). The alkoxide precursor $[\text{Rh}(\text{OEt})(\text{cod})]_2$ was prepared *in situ* by the reaction of $[\text{RhCl}(\text{cod})]_2$ with NaOEt in MeOH at room temperature.¹⁵ $[\text{Rh}(\text{OEt})(\text{cod})]_2$ was then added to a suspension of the bitriazolium salt **6** in THF at -78 °C, and the mixture was allowed to reach room temperature overnight. Upon recrystallization with $\text{CH}_2\text{Cl}_2/\text{Et}_2\text{O}$, the bis-Rh(I) species **9** (Scheme 1) was isolated rather than the expected chelate Rh(I) complex. The reaction was also performed by deprotonation of the triazolium salt with $^t\text{BuOK}$ in THF at -78 °C with subsequent addition of the metal precursor $[\text{RhCl}(\text{cod})]_2$, but the yield of **9** in the reaction decreased dramatically for reasons discussed below.

A signal at 185.2 ppm in the ^{13}C NMR spectrum of **9**, with a $^1J_{\text{Rh}-\text{C}}$ coupling constant of 50 Hz, is characteristic of a Rh(I) complex. The observed bitz/cod ratio obtained from ^1H NMR integration along with the positive ion ES-MS signal at 713.5 *m/z* confirmed the formation of the binuclear complex. The molecular structure of complex **9**, determined by single-crystal X-ray diffraction, is depicted in Figure 1, along with the principal bond lengths and angles. The structure confirms the presence of binuclear square-planar Rh(I) complex. The Rh–C distances for the carbene carbon atoms, 1.995 and 2.000 Å, are unexceptional.^{12,16}

The formation of this 2:1 M:L complex **9** is consistent with the generalization previously developed by Mata et al.,¹⁷ who found that a chelating Rh(I)-cod complex was only formed if the linker length was such as to permit each azole ring to adopt an out-of-square-plane conformation. Only with this conformation can the azole avoid a steric clash with the adjacent cod vinyl hydrogens. In such a case, a bridging structure of type **1**

(8) Bartlett, R. K.; Humphrey, I. R. *J. Chem. Soc. (C)* **1967**, 1664.
 (9) Martin, D.; Baceiredo, A.; Gornitzka, H.; Schoeller, W. W.; Bertrand, G. *Angew. Chem., Int. Ed.* **2005**, *44*, 1700.
 (10) Poyatos, M.; McNamara, W.; Incarvito, C.; Peris, E.; Crabtree, R. H. *Chem. Comm.* **2007**, 2267.
 (11) Castellanos, M. L.; Llinas, M.; Bruix, M.; Demendoza, J.; Martin, M. R. *J. Chem. Soc., Perkin Trans.* **1985**, 1209.
 (12) Poyatos, M.; Sanau, M.; Peris, E. *Inorg. Chem.* **2003**, *42*, 2572.

(13) (a) Viciano, M.; Mas-Marza, E.; Poyatos, M.; Sanau, M.; Crabtree, R. H.; Peris, E. *Angew. Chem., Int. Ed.* **2005**, *44*, 444. (b) Grundemann, S.; Albrecht, M.; Kovacevic, A.; Faller, J. W.; Crabtree, R. H. *J. Chem. Soc., Dalton Trans.* **2002**, 2163.

(14) Gade, L. H.; Cesar, V.; Bellemin-Laponnaz, S. *Angew. Chem., Int. Ed.* **2004**, *43*, 1014.

(15) Burling, S.; Field, L. D.; Li, L. H.; Messerle, B. A.; Tuner, P. *Eur. J. Inorg. Chem.* **2003**, 3179.

(16) Poyatos, M.; Mas-Marza, E.; Mata, J. A.; Sanau, M.; Peris, E. *Eur. J. Inorg. Chem.* **2003**, 1215.

(17) Mata, J. A.; Chianese, A. R.; Miecznikowski, J. R.; Poyatos, M.; Peris, E.; Faller, J. W.; Crabtree, R. H. *Organometallics* **2004**, *23*, 1253.

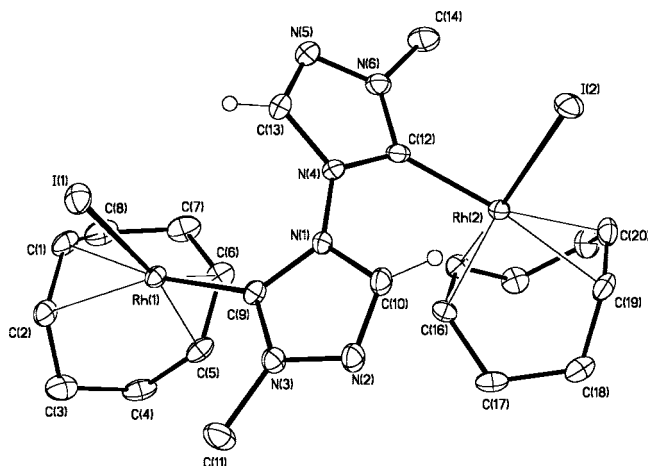
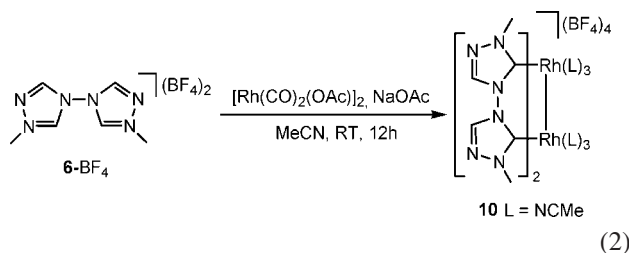


Figure 1. Molecular structure of **9**. Nonaromatic hydrogen atoms are omitted for clarity. Selected bond lengths (Å) and angles (deg): Rh(1)–C(9) 1.995(3), Rh(2)–C(12) 2.000(3), Rh(1)–C(1) 2.231(3), Rh(1)–C(2) 2.196(3), Rh(1)–C(6) 2.108(3), Rh(1)–C(5) 2.131(3), Rh(2)–C(15) 2.135(3), Rh(2)–C(16) 2.103(3), Rh(2)–C(19) 2.218(3), Rh(2)–C(20) 2.197(3); C(9)–N(1)–N(4)–C(12).

(Chart 1) is adopted in which each azole can take up such an orientation. This preferred out-of-plane conformation is indeed adopted in our 2:1 complex as shown in Figure 1.

In another attempt to coordinate the bitz ligand in chelate form to Rh(I), we carried out the reaction using a dicarbonyl precursor. The Rh(CO)₂ fragment is much less sterically hindered than Rh(cod); we therefore expected to be able to isolate [(bitz)Rh(CO)₂]⁺ since CO should be capable of allowing an in-plane conformation of the azole rings. Under strict air- and halide-free conditions, we performed the reaction of the tetrafluoroborate salt of **6** (**6**-BF₄) with [Rh(CO)₂(OAc)]₂ in the presence of NaOAc. Upon recrystallization from CH₂Cl₂/Et₂O, an unexpected metal–metal bonded dirhodium(II) complex **10** (eq 2) was isolated as a bright yellow solid. Even though dirhodium(II) complexes have been very well studied and numerous examples are known, compound **10** represents the first example bearing an NHC ligand and also the first example with a six-membered metallacycle ring. The molecular structure of **10**, also reported in the communication,¹⁰ shows that the rhodium atoms adopt an octahedral geometry with two bridging bitz ligands forming two six-membered metallacycle rings. Three coordination sites of each rhodium are occupied by MeCN. The Rh–Rh distance of 2.65 Å is consistent with the presence of a Rh–Rh bond, and 18e rule considerations suggest that this bond is single.



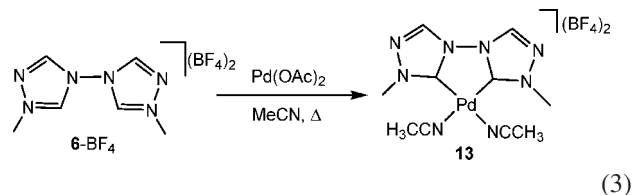
Further attempts to coordinate the bitz ligand to Rh(I) in a chelate mode were unsuccessful, consistent with the conclusions of previous work.¹⁷ The bitz ligand represents the extreme case of a short linker between the azole rings; its chelate coordination would force the ligand into the very sterically crowded complex square plane and is thus disfavored.

Synthesis and Characterization of Ruthenium(II) Complexes **11 and **12**.** The coordination of bitz to Ru via the bitrizolium salt **6** was achieved only with an external mild base. The reaction of **6** with [(η^6 -*p*-cymene)RuCl₂]₂ in MeCN in the presence of NaOAc and NaBF₄ afforded a mixture of the chelate complex [(η^6 -*p*-cymene)RuI(bitz)]BF₄ and binuclear species [(η^6 -*p*-cymene)₂Ru₂Cl₂(μ -Cl)(μ -bitz)]BF₄, **11** and **12**, respectively (Scheme 2). Arene complexes **11** and **12** were easily separated by column chromatography on silica gel. Elution with 50:50 (v/v) CH₂Cl₂/acetone allowed separation of each cationic complex as air- and moisture-stable solids. In an attempt to find conditions to obtain only one of the complexes selectively in the reaction itself and therefore enhance the yields, transmetalation from a silver(I)-NHC complex was employed as an alternative metalation strategy. Even though this procedure also gave good results, a mixture of **11** and **12** was again isolated. The new complexes were characterized by NMR and mass spectroscopy and gave satisfactory elemental analysis. In particular, ¹³C NMR signals due to the metalated carbene-carbon were seen in the typical NHC carbene region (178.5 ppm for **11** and 182.6 ppm for **12**), as well as sharp signals attributed to the aromatic protons of the arene ligand.

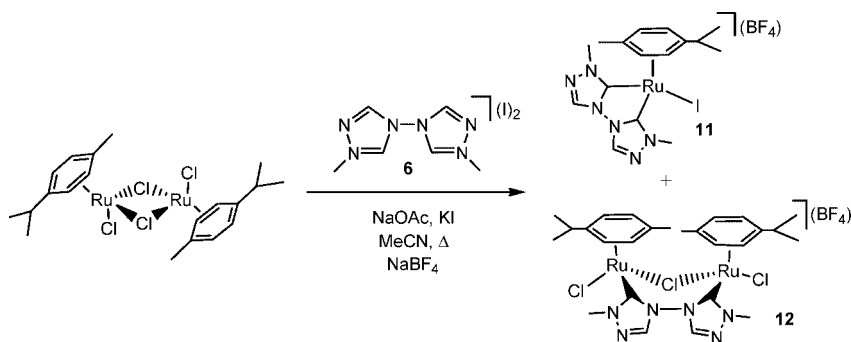
The details of the molecular structure of both cationic complexes were established by X-ray diffraction studies. Suitable crystals were isolated upon diffusion of Et₂O into a CH₂Cl₂ solution of the corresponding compound. The molecular structures of the cations of complexes **11** and **12** are depicted in Figures 2 and 3, respectively, along with selected bond distances and angles.

The molecular structure of complex **11** shows that the ruthenium atom adopts a three-legged piano stool conformation. The chelate carbene ligand has a typical acute bite angle of 76.8°. The triazole rings are almost coplanar, as reflected by the appropriate dihedral angle [C(14)–N(4)–N(1)–C(11) = 4.8°]. The coordination sphere about ruthenium is completed by a η^6 -*p*-cymene and an iodo ligand. The Ru–C_{carbene} distances of 2.019 and 2.014 Å lie within the normal range. As shown in Figure 3, the two ruthenium atoms of **12** are connected by bridging chloro and bitz ligands. The molecular structure of **12** shows both ruthenium atoms in a piano stool configuration. The Ru–C_{carbene} distances of 2.046 and 2.054 Å again lie in the typical range. This is a rare example of a bridging NHC in a dimetallic ruthenium compound. The two triazole heterocycles are mutually perpendicular, as shown by the dihedral angle [C(1)–N(1)–N(4)–C(14) = 90.2°].

Synthesis and Characterization of Palladium(II) Complex **13.** Pd(OAc)₂ was treated with the trifluoroborate salt of **6** (**6**-BF₄) in refluxing MeCN for 3 h. On removal of the volatiles, chelate complex **13** (eq 3) precipitated in pure form as a white solid. Both the ¹H and ¹³C NMR spectra were consistent with the proposed structure. In particular, the ¹³C NMR spectrum for **13** showed a signal due to the carbene carbon, at a typical value (148.1 ppm).



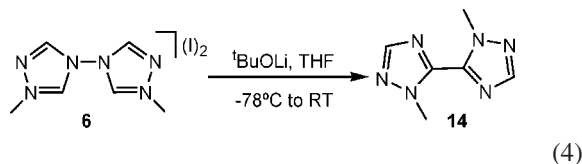
Slow diffusion of Et₂O into a MeCN solution of **13** afforded crystals suitable for X-ray diffraction. Figure 4 shows the molecular structure of the cation of **13**, along with the principal

Scheme 2. Synthesis of Chelate and Dimetallic Ru(II)-Arene Complexes **11** and **12**

bond distances and angles. As shown by the ORTEP diagram, the geometry about the palladium is square planar. The bitriazole ligand is chelating with a bite angle of 79.15° , the remaining coordination sites being occupied by MeCN. The bitriazole rings are almost coplanar, as reflected by a dihedral angle $C(1)-N(1)-N(4)-C(4)$ of 3.1° .

Rearrangement of bitriazole with Strong Base. In an attempt to use the free bis-carbene ligand in syntheses, we deprotonated the triazolium salt **6** with $t\text{BuOLi}$ in THF at -78°C (eq 4). In no case was it possible to use this method to transfer bitriazole to metal precursors. We therefore repeated the reaction in the absence of metal precursor to see if the bitriazole precursor salt **6** decomposed. Under these conditions, an unexpected rearrangement was observed. The isolated solid was air and moisture stable, allowing its purification by column chromatography. The ^1H and ^{13}C NMR spectra of the purified product displayed a very symmetrical set of signals but did not lead to a secure identification. Suitable crystals for X-ray diffraction were isolated by recrystallization from MeCN. The molecular structure (Figure 5) identifies the rearrangement product as the previously unreported C–C linked bipyrazole, **14**. This ligand rearrangement with strong base helps to explain the low yields observed in the synthesis of the di-Rh(I) dimetallic complex **9** (Scheme 1), where $t\text{BuOK}$ was employed for the deprotonation of **6**.

The same rearrangement product was observed when using a non-nucleophilic base such as $\text{KN}(\text{SiMe}_3)_2$. This rearrangement shows that the directly linked bitriazole system does not prevent base-induced decomposition as we had hoped. However, this does not imply a serious limitation to the use of the ligand because, as mentioned before, it readily coordinates to different metals in the presence of a weak base or even in the absence of it. No such rearrangement was so far observed in any bitriazole complexes, however, so once the complexation is achieved, the system seems to be stable to base.



As shown by the ORTEP diagram of **14** (Figure 5), the molecule presents a crystallographic center of inversion that bisects the $C(1)-C(1A)$ bond. The two triazole rings are coplanar, as shown by $N(1)-C(1)-C(1A)-N(3A)$ and $N(3)-C(1)-C(1A)-N(1A)$ dihedral angles of 0° .

In order to clarify whether the ligand rearrangement goes via an intra- or intermolecular mechanism, we performed the deprotonation under the same conditions using an equimolar

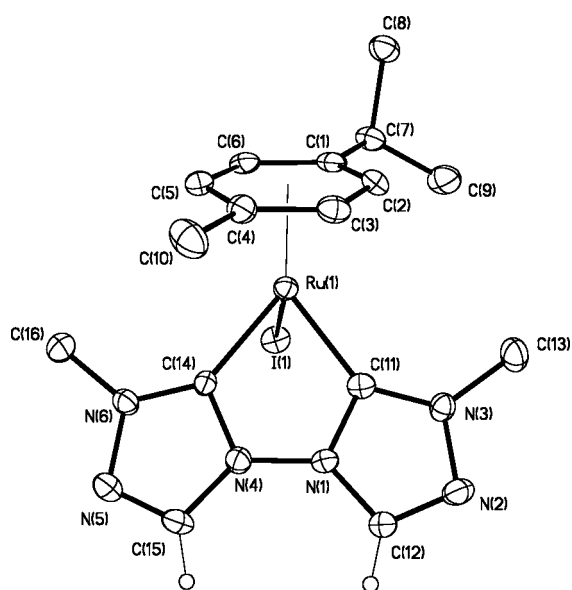


Figure 2. Molecular structure of the cation of **11**. Nonaromatic atoms are omitted for clarity. Selected bond lengths (\AA) and angles (deg): $\text{Ru}(1)-\text{Ct}$ 1.761(7), $\text{Ru}(1)-\text{C}(14)$ 2.019(7), $\text{Ru}(1)-\text{C}(11)$ 2.014(8); $\text{C}(14)-\text{Ru}(1)-\text{C}(11)$ $76.8(3)$, $\text{C}(14)-\text{Ru}(1)-\text{I}(1)$ $82.1(2)$, $\text{C}(14)-\text{N}(4)-\text{N}(1)-\text{C}(11)$ 4.8 . (Ct = arene centroid).

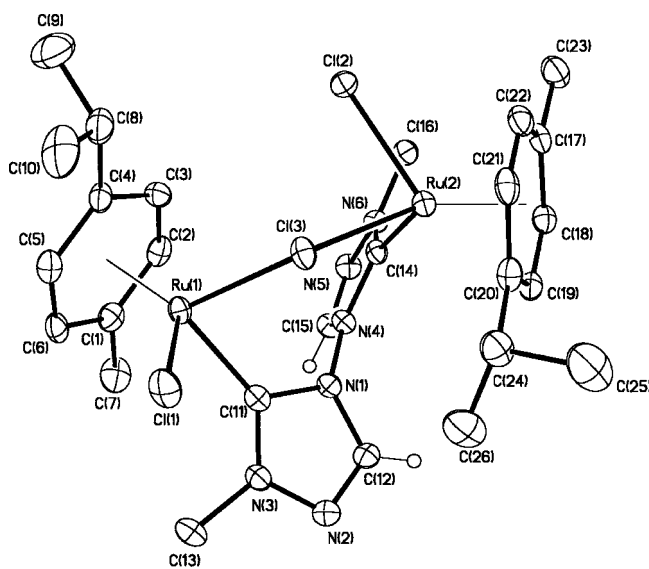


Figure 3. Molecular structure of the monocation **12**. Nonaromatic hydrogen atoms are omitted for clarity. Selected bond lengths (\AA) and angles (deg): $\text{Ru}(1)-\text{C}(1)$ 2.046(4), $\text{Ru}(2)-\text{C}(14)$ 2.054(3), $\text{Ru}(1)-\text{Cl}(3)$ 2.4450(11), $\text{Ru}(2)-\text{Cl}(3)$ 2.4076(12), $\text{Ru}(1)-\text{Ct}(1)$ 1.690, $\text{Ru}(2)-\text{Ct}(2)$ 1.698; $\text{C}(11)-\text{N}(1)-\text{N}(4)-\text{C}(14)$ 90.2 , $\text{Ru}(2)-\text{Cl}(3)-\text{Ru}(1)$ $126.43(4)$.

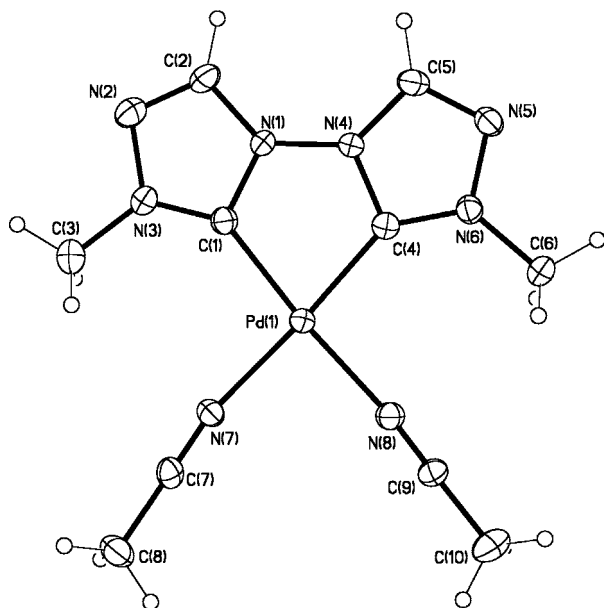


Figure 4. Molecular diagram of the cation of **13**. Selected bond lengths (Å) and angles (deg): Pd(1)–C(1) 1.986(5), Pd(1)–C(4) 1.974(4), Pd(1)–N(8) 2.039(4), Pd(1)–N(7) 2.044(3); C(1)–Pd(1)–C(4) 79.15(18), C(1)–N(1)–N(4)–C(4) 3.1.

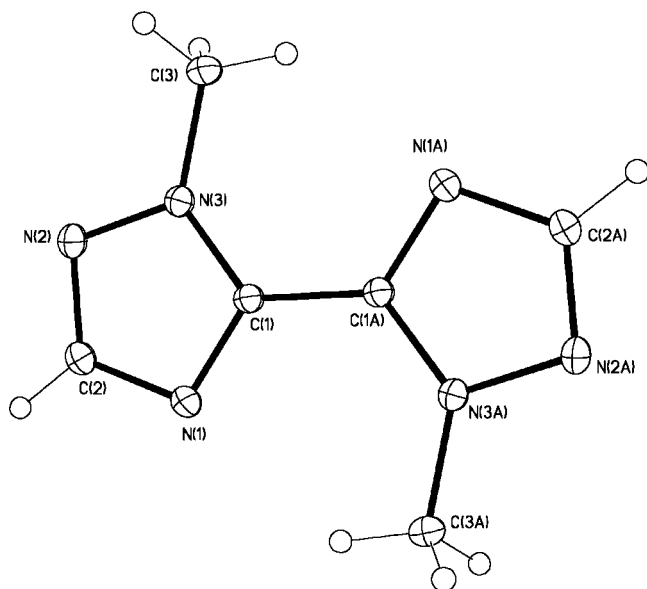
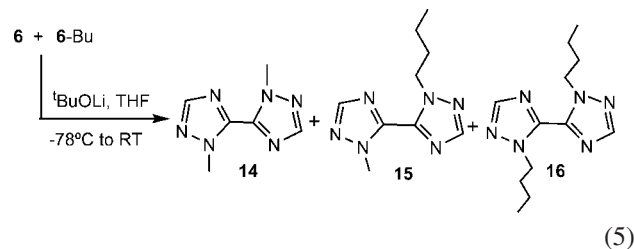


Figure 5. Molecular structure of **14**. Selected bond lengths (Å) and angles (deg): C(1)–C(1A) 1.461(4), C(1)–N(1) 1.336(2), N(1)–C(2) 1.354(3), C(2)–N(2) 1.318(3), N(2)–N(3) 1.357(2), N(3)–C(1) 1.348(2), N(3)–C(3) 1.460(2); C(1)–N(1)–C(2) 102.37(17), C(2)–N(2)–N(3) 103.04(15), C(1)–N(3)–N(2)–109.09(17), N(1)–C(1)–N(3) 110.30(16), N(1)–C(1)–C(1A) 125.0(2), N(3)–C(1)–C(1A) 124.7(2), N(2)–C(2)–N(1) 115.20(18).

mixture of *N*-methyl precursor salt **6** and its *n*-butyl counterpart, 1,1'-di-*n*-butyl-4,4'-bi-1,2,4-triazolium iodide (**6-Bu**). After flash chromatography on silica gel, three different rearrangement products were isolated and characterized by ¹H and ¹³C NMR. The three isolated products were identified as **14**, **15**, and **16** (eq 5). This result clearly indicates that the mechanism of the process is intermolecular, since the crossover product with methyl and *n*-butyl wingtips (**15**) is formed. Further work on the mechanism is currently in progress.



Ligand Electronic Properties. Typical N-heterocyclic carbene (NHCs) ligands tend to be much more strongly donor than phosphines or amines, as would be expected from the very basic character of the free NHC. The bitz ligand embodies two factors that might be expected to lead to a lower donor power than typical NHCs, however. It is a triazole rather than an imidazole-based NHC, and the extra electronegative nitrogen atom in each azole ring is known to lead to a significantly lower donor power. The two azole rings are also delocalized because the inter-ring N–N bond is short, e.g., 1.379 and 1.374 Å for chelate complexes **13** and **7** and 1.378 and 1.386 Å for dimetallic species **12** and **9**, corresponding to a bond order between 1 and 2. Each azole ring may therefore act as an electron-withdrawing substituent with respect to the other.

DFT calculations were previously used to estimate⁵ Tolman electronic parameters of ligands from the highest $\nu(\text{CO})$ infrared stretching frequency values in each of the members of the series of $\text{LNi}(\text{CO})_3$ compounds according to the Tolman procedure.¹⁸ The data obtained computationally showed exceptionally good agreement with experiment for a wide range of L after a scaling factor (0.96) was uniformly applied. The resulting data also showed good agreement with Lever parameters, typically used in coordination chemistry work.

It is not possible to estimate electronic parameters for chelating ligands from $\nu(\text{CO})$ values of the corresponding monodentate $\text{LNi}(\text{CO})_3$, unless the assumption is made that the chelating ligand has the same electronic parameter as a monodentate model ligand (e.g., MePPH_2 modeling dppe). This assumption has not been previously tested, however.

In other prior work,¹⁹ we showed that Tolman-like electronic parameters for chelating ligands could be reliably obtained from $\nu(\text{CO})$ values of chelating $(\text{L}-\text{L})\text{Mo}(\text{CO})_4$ or bis-monodentate *cis*- $(\text{L})_2\text{Mo}(\text{CO})_4$ compounds after application of a conversion equation from the Mo to the Ni scale, the two scales giving a very satisfactory mutual correlation. Because the Mo precursor carbonyl $\text{Mo}(\text{CO})_6$ is very much more convenient to handle than $\text{Ni}(\text{CO})_4$, this approach provides a substantial added experimental convenience.

Combining these two approaches, we have now calculated the electronic parameters for bitz and a number of related ligands to probe these questions. The ligands and $\nu(\text{CO})$ values of $(\text{L}-\text{L})\text{Mo}(\text{CO})_4$ or *cis*- $(\text{L})_2\text{Mo}(\text{CO})_4$ are shown in Table 1. The raw $\nu(\text{CO})$ values are used for the discussion that follows.

For ethylene-bridged diphosphines, the assumption that the electronic effect of the model monomer can be taken as the correct value for the chelate does indeed hold. PMe_3 (2103.6 cm^{-1}) is very close to $\text{Me}_2\text{PCH}_2\text{CH}_2\text{PMe}_2$ (2104.6 cm^{-1}) in

(18) Tolman, C. A. *Chem. Rev.* **1977**, *77*, 313.

(19) Anton, D. R.; Crabtree, R. H. *Organometallics* **1983**, *2*, 621.

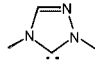
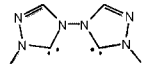
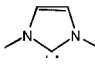
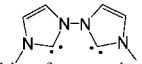
(20) Mukerjee, S. L.; Nolan, S. P.; Hoff, C. D.; Delavega, R. L. *Inorg. Chem.* **1988**, *27*, 81.

(21) Overton, C.; Connor, J. A. *Polyhedron* **1982**, *1*, 53.

(22) Frey, G. D.; Ofele, K.; Krist, H. G.; Herdtweck, E.; Herrmann, W. A. *Inorg. Chim. Acta* **2006**, *359*, 2622.

(23) Kreiter, C. G.; Ofele, K.; Wieser, G. W. *Chem. Ber.* **1976**, *109*, 1749.

Table 1. Experimental and Computed Carbonyl Stretching Frequencies for Complexes (L–L)Mo(CO)₄ or *cis*-(L)₂Mo(CO)₄

L	$\nu(\text{CO})_{\text{exp}}$ (solvent, cm ⁻¹)	ref.	$\nu(\text{CO})_{\text{comp}}$ (cm ⁻¹)	$\nu(\text{CO})_{\text{scaled}}$ (cm ⁻¹) ^a	TEP _{estimated} (cm ⁻¹) ^b
PMe ₃	2036 (THF)	20	2103.6	2019.4	2068.5
Me ₂ PCH ₂ CH ₂ PMe ₂ (dmpe)	2020 (THF)	20	2104.6	2020.4	2069.1
pyridine	2015 (THF)	20	2103.1	2018.9	2068.2
2,2'-dipyridyl (dippy)	2039 (THF)	20	2107.0	2022.7	2070.5
pyrimidine	not isolated	-	2107.1	2022.8	2070.5
2,2'-bipyrimidyl (bpym)	2023 (MeCN)	21	2110.7	2026.3	2072.6
	2000 (THF)	22	2090.8	2007.2	2061.3
	not isolated	this work	2109.7	2025.3	2072.1
	1984 (C ₆ H ₆)	23	2083.0	1999.7	2056.8
	not isolated	-	2100.3	2016.3	2066.7

^a Scaled carbonyl stretching frequencies by a factor of 0.96. ^b Calculated using the equation in ref 19: $\nu_{\text{Ni}} = 0.593\nu_{\text{Mo}} + 871$.

$\nu(\text{CO})$ value, with a negligible chelate shift of only +1 cm⁻¹. The same holds for dipy, even though the possibility now exists for electronic communication between the rings via π -delocalization. Pyridine (2103.1 cm⁻¹) is still very close to 2,2'-dipyridyl (2107.0 cm⁻¹) in $\nu(\text{CO})$ value, with a small chelate shift of +3.9 cm⁻¹. Pyrimidine (2107.1 cm⁻¹) and 2,2'-dipyrimidyl (2110.7 cm⁻¹) behave the same way with a small chelate shift of +3.6 cm⁻¹.

With bitz (2109.7 cm⁻¹), we have a very different situation. If we take the corresponding 1,4-dimethyl-1,2,4-triazole-5-ylidene (2090.8 cm⁻¹), we find a chelation shift of 18.9 cm⁻¹. Such a choice of monodentate model would lead to a severely erroneous conclusion about the donor power of the chelate. This illustrates the value both of the computational approach in which appropriate series can be rapidly screened and of the (L–L)Mo(CO)₄/*cis*-(L)₂Mo(CO)₄ test bed. A similar shift (+17.3 cm⁻¹) holds for the hypothetical bis-imidazole-2,2'-ylidene (2100.3 cm⁻¹), versus the analogous model monodentate NHC (2083.0 cm⁻¹).

This large chelate shift presumably indicates that each azole ring is indeed a substantial electron-acceptor substituent relative to the other ring and that a combination of decreased σ -donor power and enhanced π -acceptor power may combine to give bitz a net donor power that is exceptionally low for an NHC. The computed values suggest that bitz is a less strong donor than either dmpe or dipy. Since phosphines are the ligand class with the most applicability in organometallic catalysis and dipy is widespread in coordination catalysis, a chelating NHC with an electron-donor power in this range could be of substantial interest.

To extract the Tolman electronic parameters (TEPs) for the ligands in Table 1, we have compared the experimental values with the computations for the range of L to find what scaling factor should be applied. A value of 0.96 again seems appropriate, leading to the scaled $\nu(\text{CO})$ values shown in the table.

Finally, we apply the conversion equation from the Mo to the Ni scale reported in the literature¹⁹ to obtain the estimated Tolman electronic parameters of the ligands also shown in the table. Attempts to make the Mo(CO)₄(bitz) complex experimentally all failed, emphasizing the value of the computational approach.

Catalytic Properties. Hydrogen Transfer. Some of the bitz complexes showed good catalytic activity for reduction of C=O and C=N groups via hydrogen transfer from ¹PrOH. All the catalytic runs were carried out in refluxing ¹PrOH, under inert atmosphere and using ¹BuOK as cocatalyst. Under these conditions, both mono- and bis-chelate Rh(III) complexes **7** and **8** (Scheme 1) catalyze the reduction of ketones. Complex **7** (1 mol %) catalyzes the reduction of acetophenone, cyclohexanone, benzophenone, and benzylidene aniline, giving quantitative yields after a few hours. The observed yields in the hydrogenation of aromatic ketones are similar to those observed with other chelated Rh(III) bicarbene complexes reported by our group.²⁴ Although complex **7** also performed well as hydrogen transfer catalyst for aliphatic ketones, the rates were slower than those observed for the Rh(III) complexes mentioned above. Table 2 shows selected data for transfer hydrogenation from ¹PrOH/¹BuOK using complexes **7** and **8** as catalysts.

Conclusions

The bitz ligand proves to be useful in having a wide applicability to late transition metals. In particular, an unusual di-Rh(II) complex has been isolated. Remarkably, it readily coordinates to Rh(III) in the absence of an external base, giving a monochelate species. By computational studies, we have

(24) Albrecht, M.; Crabtree, R. H.; Mata, J.; Peris, E. *Chem. Commun.* **2002**, 32.

Table 2. Selected Results on Catalytic Reduction of C=O and C=N Groups via Hydrogen Transfer from ⁱPrOH/^tBuOK at 82 °C

entry	catalyst	substrate	time (h)	cat. loading (mol %)	yield (%) ^a	TON ^b
1	7	acetophenone	3	1	>98	98
2	7	acetophenone	12	0.1	>98	980
3	7	benzophenone	6	1	>98	98
4	7	benzophenone	24	0.1	25	250
5	7	benzylidene aniline	6	1	90	90
6	7	cyclohexanone	48	1	>98	98
7	7	cyclohexanone	48	0.1	40	400
8	8	acetophenone	7	1	>98	98
9	8	benzophenone	5	1	>98	98
10	8	benzylidene aniline	24	1	70	70
11	8	cyclohexanone	6	1	>98	98

^a Yields were determined by ¹H NMR spectroscopy, using 1,3,5-methoxybenzene as internal standard. ^b TON = (mmol of product)/(mmol of catalyst).

proved its very low electron-donor power for a chelating NHC, comparable with those of dmpe and dipy. In an unexpected rearrangement, the bitz precursor salt converts to a new C–C linked bitriazole. As we have seen, a minor drawback to the bitz precursor is its rearrangement in the presence of strong bases, although weak bases are perfectly tolerated. It can however be incorporated into a variety of complexes under neutral conditions, perhaps because of the more strongly acidic character of bitz compared to typical NHCs. Once bound, it is completely stable to rearrangement, thus providing a versatile access to a wide variety of bitz derivatives. Some of the new complexes performed well as hydrogen transfer catalysts.

Experimental Section

General Procedures. All operations were carried out using standard Schlenk techniques under nitrogen. All NMR spectra were recorded at room temperature on Bruker spectrometers operating at 400 or 500 MHz (¹H NMR) and 100 or 125 MHz (¹³C NMR), respectively, and referenced to the residual proton solvent (¹H) or solvent (¹³C) resonance. [(*η*⁶-*p*-cymene)RuCl₂]₂,²⁵ PdCl₂(cod),²⁶ [Rh(OEt)(cod)]₂,¹⁵ [Rh(CO)₂(OAc)]₂,²⁷ 4,4'-bi-1,2,4-triazole,⁷ and precursor **6**¹¹ were prepared as reported in the literature. THF was purified and dried by standard methods. All other reagents were used as received from commercial suppliers. Microanalyses were carried out by Atlantic Microlabs, Inc. (Norcross, GA). Electrospray mass spectra (ESI-MS) were recorded on a Micromass ZQ instrument using nitrogen as drying agent and nebulizing gas.

Synthesis of 1,1'-Dimethyl-4,4'-bi-1,2,4-triazolium Tetrafluoroborate, 6-BF₄. 4,4'-Bi-1,2,4-triazole (300 mg, 2.2 mmol) and trimethylxonium tetrafluoroborate (718 mg, 4.85 mmol) were placed together in a round-bottom flask and suspended in 10 mL of MeCN; the mixture was heated at reflux overnight. The desired salt was collected by filtration, washed several times with CH₂Cl₂, and dried under vacuum. Yield: 710 mg (95%). ¹H NMR (400 MHz, DMSO-*d*₆): δ 10.70 (s, 2H, NCHN), 9.74 (s, 2H, NCHN), 4.40 (s, 6H, CH₃). ¹³C NMR (125 MHz, CD₃CN): δ 142.9 (NCHN), 40.4 (NCH₃). Anal. Calcd for C₆H₁₀N₆B₂F₈ (339.79): C, 21.21; H, 2.97; N, 24.73. Found: C, 21.20; H, 2.92; N, 24.46.

Synthesis of 1,1'-Di(n-butyl)-4,4'-bi-1,2,4-triazolium Diiodide, 6-Bu. 4,4'-Bi-1,2,4-triazole (500 mg, 3.5 mmol) and 1-iodobutane (2 mL) were dissolved in 10 mL of MeCN. The mixture was heated at 100 °C in a sealed tube overnight, yielding a yellow solid, which

was collected by filtration and washed twice with acetone. Yield: 1.3 g (72%). ¹H NMR (400 MHz, DMSO-*d*₆): δ 10.78 (s, 2H, NCHN), 9.77 (s, 2H, NCHN), 4.68 (t, ³J_{H–H} = 6.9 Hz, 4H, NCH₂), 1.93 (m, 4H, CH₂(n-Bu)), 1.42 (m, 4H, CH₂(n-Bu)), 0.98 (t, ³J_{H–H} = 7.3 Hz, 6H, CH₃(n-Bu)). ¹³C NMR (100 MHz, DMSO-*d*₆): δ 144.1 (NCHN), 143.6 (NCHN), 52.6 (NCH₂), 30.0 (CH₂(n-Bu)), 18.6 (CH₂(n-Bu)), 13.3 (CH₃(n-Bu)). Anal. Calcd for C₁₂H₂₂N₆I₂ (504.15): C, 28.59; H, 4.40; N, 16.67. Found: C, 28.86; H, 4.40; N, 16.74.

Synthesis of [(bitz)RhI₃(CH₃CN)], 7. A mixture of [RhCl(cod)]₂ (100 mg, 0.20 mmol), precursor **6** (169 mg, 0.40 mmol), and KI (67 mg, 0.40 mmol) was heated at 50 °C in degassed MeCN for 3 h under inert atmosphere. The suspension was then filtered through Celite and the solvent removed under high pressure. The crude solid was purified by column chromatography. Elution with a mixture of CH₂Cl₂/acetone (1:1 (v/v)) afforded a red band containing compound **7**, which was recrystallized in MeCN. Suitable crystals for X-ray diffraction studies were grown by slow evaporation of a MeCN solution of **7**. Yield: 200 mg (71%). ¹H NMR (400 MHz, DMSO-*d*₆): δ 9.77 (s, 1H, NCHN), 9.75 (s, 1H, NCHN), 4.54 (s, 3H, NCH₃), 4.27 (s, 3H, NCH₃), 3.39 (s, 3H, NCH₃). ¹³C NMR (125 MHz, DMSO-*d*₆): δ 166.5 (d, ¹J_{Rh–C} = 42.4 Hz, Rh–C_{carbene}), 158.2 (d, ¹J_{Rh–C} = 43.8 Hz, Rh–C_{carbene}), 134.3 (NCHN), 133.9 (NCHN), 116.8 (CH₃CN), 42.3 (NCH₃), 38.5 (NCH₃), 28.5 (CH₃CN). MS(ESI) *m/z* (%): 521.3 (100) [M – I – CH₃CN]⁺. Anal. Calcd for C₈H₁₁I₃N₇Rh (688.84)·CH₃CN: C, 16.45; H, 1.93; N, 15.35. Found: C, 16.14; H, 1.98; N, 15.95.

Synthesis of cis-[(bitz)₂RhI₂][I], 8. A mixture of [RhCl(cod)]₂ (100 mg, 0.20 mmol), precursor **6** (334 mg, 0.8 mmol), NaOAc (100 mg, 1.2 mmol), and KI (100 mg, 0.6 mmol) was stirred at room temperature for 48 h in MeCN under inert atmosphere. Afterward, the suspension was filtered through Celite and the solvent removed under vacuum. The resulting orange residue was washed several times with a mixture of CH₂Cl₂/MeCN (9:1 (v/v)), giving the desired compound as a pale yellow solid. Suitable crystals for X-ray diffraction were obtained by slow diffusion of Et₂O into a MeCN solution of **8**. Yield: 180 mg (55%). ¹H NMR (500 MHz, CD₃CN): δ 9.98 (s, 2H, NCHN), 9.75 (s, 2H, NCHN), 4.67 (s, 6H, NCH₃), 3.46 (s, 6H, NCH₃). ¹³C NMR (125 MHz, CD₃CN): δ 167.6 (d, ¹J_{Rh–C} = 34.9 Hz, Rh–C_{carbene}), 162.7 (d, ¹J_{Rh–C} = 43.6 Hz, Rh–C_{carbene}), 135.5 (NCHN), 135.0 (NCHN), 42.3 (NCH₃), 38.9 (NCH₃). MS(ESI) *m/z* (%): 685.3 (80) [M]⁺, 559.6 (20) [M – I]⁺. Anal. Calcd for C₁₂H₁₆I₃N₇Rh (811.95): C, 17.75; H, 1.99; N, 20.70. Found: C, 17.80; H, 2.05; N, 21.10.

Synthesis of [(μ-bitz){RhI(cod)}₂], 9. A solution of [RhCl(cod)]₂ (100 mg, 0.20 mmol) in MeOH (0.6 mL) was treated with NaOEt (0.44 mmol, 127 μL solution 21 wt % NaOEt in EtOH) under nitrogen. After stirring for 1 h, the pale yellow solid was collected by filtration and washed with MeOH. [Rh(OEt)(cod)]₂ was then added to a suspension of the precursor **6** (0.343 mmol, 144 mg) in THF (10 mL) at –78 °C. The mixture was allowed to reach room temperature overnight. Compound **9** was isolated as a yellow solid after recrystallization of the crude from CH₂Cl₂/Et₂O. Suitable crystals for X-ray diffraction were grown by slow diffusion of Et₂O into a solution of the compound in CH₂Cl₂. Yield: 120 mg (67%). ¹H NMR (400 MHz, CDCl₃): δ 10.36 (s, 2H, NCHN), 5.39 (m, 8H, CH₂cod), 4.26 (s, 6H, NCH₃), 1.61–2.50 (m, 16H, CH₂cod). ¹³C NMR (125 MHz, CDCl₃): δ 185.2 (d, ¹J_{Rh–C} = 50 Hz, Rh–C_{carbene}), 141.2 (NCHN), 100.1 (d, ¹J_{Rh–C} = 7.5 Hz, Rh–C_{cod}), 99.8 (d, ¹J_{Rh–C} = 7.5 Hz, Rh–C_{cod}), 73.1 (d, ¹J_{Rh–C} = 12.5 MHz, Rh–C_{cod}), 72.1 (d, ¹J_{Rh–C} = 12.5 MHz, Rh–C_{cod}), 41.9 (NCH₃), 33.06, 32.91, 29.91, 29.45 (CH₂cod). MS(ESI) *m/z* (%): 713.5 (100) [M – I]⁺. Anal. Calcd for C₂₂H₃₂I₂N₆Rh₂ (840.16): C, 31.45; H, 3.84; N, 10.00. Found: C, 31.52; H, 3.79; N, 9.97.

Synthesis of [Rh(μ-bitz)(CH₃CN)₃]₂[BF₄]₄, 10. [Rh(CO)₂(OAc)]₂ (75 mg, 0.17 mmol), precursor **6-BF₄** (116 mg, 0.34 mmol), and NaOAc (28.2 mg, 0.34 mmol) were placed together

(25) Bennett, M. A.; Smith, A. K. *J. Chem. Soc., Dalton Trans.* **1974**, 233.

(26) Drew, D.; Doyle, J. R. *Inorg. Synth.* **1990**, 28, 346.

(27) Wilson, J. M.; Sunley, G. J.; Adams, H.; Haynes, A. J. *Organomet. Chem.* **2005**, 690, 6089.

in a Schlenk tube, and 5 mL of degassed MeCN was added. The resulting dark red solution was stirred at room temperature for 12 h. Afterward, the suspension was filtered and the solvent removed under high pressure, giving a dark orange solid. Compound **6** was obtained as a yellow solid upon recrystallization from CH₂Cl₂/Et₂O. Suitable crystals for X-ray diffraction were obtained by slow diffusion of Et₂O into a solution of compound **10** in MeCN. Yield: 134 mg (70%). ¹H NMR (400 MHz, DMSO-*d*₆): δ 9.69 (s, 2H, NCHN), 9.54 (s, 2H, NCHN), 4.49 (s, 6H, NCH₃), 3.58 (s, 6H, NCH₃), 2.81 (s, 6H, CH₃CN), 2.35 (s, 6H, CH₃CN). ¹³C NMR (125 MHz, CD₃CN): δ 161.7 (d, ¹J_{Rh-C} = 51.1 Hz, Rh-C_{carbene}), 161.1 (d, ¹J_{Rh-C} = 53.6, Rh-C_{carbene}), 141.4 (NCHN), 139.3 (NCHN), 42.1 (NCH₃), 40.1 (NCH₃). Anal. Calcd for C₂₄H₃₄B₄F₁₆N₁₈Rh₂ (1127.69) · 2CH₂Cl₂: C, 24.07; H, 2.95; N, 19.43. Found: C, 23.44; H, 2.92; N, 20.16.

Synthesis of [(η⁶-*p*-cymene)RuI(bitz)]BF₄ (11**) and [(η⁶-*p*-cymene)₂Ru₂Cl₂(μ-Cl)(bitz)]BF₄ (**12**). Method A.** A mixture of [(η⁶-*p*-cymene)RuCl₂]₂ (150 mg, 0.24 mmol), bitriazolium salt **6** (205 mg, 0.49 mmol), NaOAc (200 mg, 2.44 mmol), and KI (200 mmol, 1.20 mmol) was refluxed in MeCN for 5 h. After cooling, the mixture was filtered through Celite and the solvent was removed under vacuum. The crude solid was purified by column chromatography. A mixture of CH₂Cl₂/acetone (9:1 (v/v)) eluted unreacted [(η⁶-*p*-cymene)RuCl₂]₂. CH₂Cl₂/acetone (1:1 (v/v)) containing NaBF₄ (50 mg, 0.45 mmol) eluted an orange band of compound **11**, followed by a red band of **12**.

Method B. A mixture of **6** (136.5 mg, 0.33 mmol) and Ag₂O (152 mg, 0.65 mmol) was stirred in MeOH at 60 °C for 1 h, and then [(η⁶-*p*-cymene)RuCl₂]₂ (100 mg, 0.32 mmol) was added. The mixture was stirred for 60 min and filtered through Celite, and the solvent was removed under vacuum. The crude solid was purified by column chromatography on silica gel. Elution with a mixture of CH₂Cl₂/acetone (9:1 (v/v)) afforded the separation of a minor red band containing unreacted [(η⁶-*p*-cymene)RuCl₂]₂. Further elution with CH₂Cl₂/acetone (1:1 (v/v)) and addition of NaBF₄ (50 mg, 0.45 mmol) afforded the elution of an orange band of **11**, followed by a red band containing **12**.

11. ¹H NMR (400 MHz, CDCl₃): δ 10.40 (s, 2H, NCHN), 6.24 (d, 2H, ³J_{H-H} = 4.8 Hz, *p*-(CH₃)₆H₄CH(CH₃)₂), 6.17 (d, 2H, ³J_{H-H} = 4.8 Hz, *p*-(CH₃)₆H₄CH(CH₃)₂), 4.30 (s, 6H, NCH₃), 2.67 (m, 1H, *p*-(CH₃)₆H₄CH(CH₃)₂), 2.49 (s, 3H, *p*-(CH₃)₆H₄CH(CH₃)₂), 1.06 (d, 6H, ³J_{H-H} = 5.5 Hz, *p*-(CH₃)₆H₄CH(CH₃)₂). ¹³C NMR (125 MHz, CDCl₃): δ 178.5 (Ru-C_{carbene}), 136.2 (NCHN), 113.2, 108.3, 92.3, 90.1 (C_{*p*}-cymene), 42.3 (NCH₃), 32.3 (CH(CH₃)₂), 23.4 (CH(CH₃)₂), 21.2 (CH₃). MS(ESI) *m/z* (%): 527.1 (100) [M]⁺. Anal. Calcd for C₁₆H₂₂F₄IN₆BRu (613.17) · CH₂Cl₂: C, 29.25; H, 3.47; N, 12.04. Found: C, 29.05; H, 3.41; N, 12.76.

12. ¹H NMR (500 MHz, CDCl₃): δ 9.37 (s, 2H, NCHN), 5.74 (d, 4H, ³J_{H-H} = 6 Hz, *p*-cymene), 5.50 (d, 2H, ³J_{H-H} = 6 Hz, *p*-cymene), 5.39 (d, 2H, ³J_{H-H} = 6.5 Hz, *p*-cymene), 4.38 (s, 6H, NCH₃), 3.09 (m, 2H, *p*-(CH₃)₆H₄CH(CH₃)₂), 2.06 (s, 6H, *p*-(CH₃)₆H₄CH(CH₃)₂), 1.22 (d, 6H, ³J_{H-H} = 7 Hz, *p*-(CH₃)₆H₄CH(CH₃)₂), 1.06 (d, 6H, ³J_{H-H} = 6.5 Hz, *p*-(CH₃)₆H₄CH(CH₃)₂). ¹³C NMR (125 MHz, CDCl₃): δ 182.6 (Ru-C_{carbene}), 146.3 (NCHN), 113.0, 98.9, 89.7, 88.6, 85.7, 83.7 (C_{*p*}-cymene), 46.7 (NCH₃), 31.5 (CH(CH₃)₂), 23.2, 21.5 (CH(CH₃)₂), 19.6 (CH₃). MS(ESI) *m/z* (%): 435.8 (30) [LRu(*p*-cymene)Cl]⁺. Anal. Calcd for C₂₆H₃₆BCl₃F₄N₆Ru₂ (827.91): C, 37.72; H, 4.38; N, 10.15. Found: C, 38.08; H, 4.47; N, 10.22.

Synthesis of [Pd(bitz)(NCCH₃)](BF₄)₂, **13.** An equimolar mixture of Pd(OAc)₂ (100 mg, 0.445 mmol) and precursor **6**-BF₄ (152 mg, 0.445 mmol) was refluxed in MeCN for 3 h. The initial orange suspension turned into a colorless solution after half an hour. After cooling and removal of the volatiles under vacuum, complex **13** was isolated as a white solid, no further purification being needed. Crystals suitable for X-ray diffraction were grown by slow diffusion of Et₂O into a MeCN solution. Yield: 200 mg (82%). ¹H NMR (500 MHz, CD₃CN): δ 9.16 (s, 2H, NCHN), 4.14 (s, 6H, NCH₃), 1.94 (s, 6H, CH₃CN). ¹³C NMR (125 MHz, CD₃CN): δ

148.1 (Pd-C_{carbene}), 134.1 (NCHN), 40.34 (NCH₃). Anal. Calcd for C₁₀H₁₄N₈PdB₂F₈ (526.30): C, 22.82; H, 2.68; N, 21.29. Found: C, 22.82; H, 2.78; N, 21.57.

Synthesis of 5,5'-Bi-1,2,4-triazole, **14.** Under inert atmosphere, bitriazolium salt **6** (146 mg, 0.35 mmol) was suspended in distilled THF (20 mL). The resulting mixture was immersed in a bath at -78 °C, and ¹BuOLi (2 equiv, 56 mg, 0.7 mmol) was added. The mixture was warmed to room temperature overnight. The beige solution was then filtered through Celite, the solvent evaporated under vacuum, and the crude solid purified by column chromatography. Elution with EtOAc afforded the separation of **14**. Yield: 44 mg (77%). ¹H NMR (400 MHz, CDCl₃): δ 7.93 (s, 2H, NCHN), 4.27 (s, 6H, NCH₃). ¹³C NMR (125 MHz, CDCl₃): δ 150.9 (NCHN), 143.8 (NCN), 38.7 (NCH₃). Anal. Calcd for C₆H₈N₆ (164.17): C, 43.90; H, 4.91; N, 51.19. Found: C, 43.12; H, 4.86; N, 47.76.

Crossover Experiment. An equimolar mixture of the bitriazolium salts **6** (75 mg, 0.179 mmol) and **6**-Bu (90 mg, 0.179 mmol) was suspended in distilled THF (20 mL). The suspension was then immersed in a bath at -78 °C, and ¹BuOLi (72 mg, 0.895 mmol) was added. The mixture was warmed to room temperature overnight. The red solution was then filtered through Celite, the solvent evaporated under vacuum, and the crude solid purified by column chromatography. Elution with a mixture of EtOAc/hexanes (4:6 (v/v)) gave separation of **16**, **15**, and **14**.

15. ¹H NMR (400 MHz, CDCl₃): δ 7.93 (s, 1H, NCHN), 7.92 (s, 1H, NCHN), 4.69 (t, ³J_{H-H} = 7.4 Hz, 2H, NCH₂), 4.25 (s, 3H, NCH₃), 1.82 (m, 2H, CH₂(*n*-Bu)), 1.28 (m, 2H, CH₂(*n*-Bu)), 0.87 (t, ³J_{H-H} = 7.3 Hz, 3H, CH₃(*n*-Bu)). ¹³C NMR (100 MHz, CDCl₃): δ 149.6 (2C, NCHN), 142.3 (NCN), 141.9 (NCN), 49.4 (NCH₂), 37.3 (NCH₃), 30.9 (CH₂(*n*-Bu)), 18.6 (CH₂(*n*-Bu)), 12.6 (CH₃(*n*-Bu)).

16. ¹H NMR (400 MHz, CDCl₃): δ 7.93 (s, 2H, NCHN), 4.67 (t, ³J_{H-H} = 7.3 Hz, 4H, NCH₂), 1.81 (m, 4H, CH₂(*n*-Bu)), 1.26 (m, 4H, CH₂(*n*-Bu)), 0.85 (t, ³J_{H-H} = 7.3 Hz, 6H, CH₃(*n*-Bu)). ¹³C NMR (400 MHz, CDCl₃): δ 149.5 (2C, NCHN), 141.9 (NCN), 49.3 (NCH₂), 31.0 (CH₂(*n*-Bu)), 18.6 (CH₂(*n*-Bu)), 12.6 (CH₃(*n*-Bu)).

Typical Procedure for Catalytic Transfer Hydrogenation. A mixture of the substrate (0.5 mmol), catalyst (1 or 0.1 mol % vs substrate), ¹BuOK (0.05 mmol, 10 mol %), and ¹PrOH (10 mL) was heated at reflux under inert atmosphere. Aliquots (0.2 mL) were taken at the desired times, quenched with pentane, and filtered through a short path of SiO₂. The filtrate was evaporated to dryness (nonvolatile substrates) and analyzed by ¹H NMR spectroscopy, using 1,3,5-trimethoxybenzene as an internal standard.

X-Ray Diffraction Study of Compounds **9, **11**, **12**, **13**, and **14**.** Crystal samples were mounted with epoxy cement on the tip of a fine glass fiber. All measurements were made on a Nonius KappaCCD diffractometer with graphite-monochromated Mo Kα radiation (λ = 0.71073 Å). Space groups were unambiguously determined based on statistical analyses of intensity distributions and the successful solution and refinement of the structures. The data were collected using omega scans with frame widths of 1.0–2.0° and a detector-to-crystal distance, D_s, of 35.0 mm. Each frame was exposed twice for the purpose of de-zingering. The data frames were processed and scaled using the DENZO software package.²⁸ The data were corrected for Lorentz and polarization effects. The structures were solved by direct methods and expanded using Fourier techniques.²⁹ The non-hydrogen atoms were refined anisotropically, and hydrogen atoms, with exceptions noted, were treated as idealized contributions. The final cycles of full-matrix

(28) Otwinowski, Z.; Minor, W. Processing of X-Ray Diffraction Data Collected in Oscillation Mode. In *Methods in Enzymology: Macromolecular Crystallography*, Part A; Carter, C. W., Jr., Sweet, R. M., Eds.; Academic Press: New York, 1997; Vol. 126.

(29) SHELXTL, v.6.12; Bruker-AXS: Madison, WI, 2001.

Table 3. X-Ray Experimental Data of Compounds 9, 11, 12, 13, and 14

	9	11	12	13	14
formula	C ₂₂ H ₃₂ I ₂ N ₆ Rh ₂	C ₁₆ H ₂₂ B _{0.20} F _{0.80} I _{1.80} N ₆ Ru	C ₂₆ H ₃₆ BCl ₃ F ₄ N ₆ Ru ₂	C ₁₁ H _{15.50} B ₂ F ₈ N _{8.50} Pd	C ₆ H ₈ N ₆
MW	840.16	645.25	827.91	546.84	164.18
temp (K)	173(2)	173(2)	173(2)	198(2)	173(2)
cryst syst	triclinic	monoclinic	monoclinic	orthorhombic	monoclinic
space group	P $\bar{1}$	P2(1)/c	C2/c	Fdd2	C2/c
a (Å)	8.7286(17)	9.4985(19)	23.418(5)	25.338(5)	15.068(3)
b (Å)	12.243(2)	8.0984(16)	15.392(3)	28.695(6)	6.8810(14)
c (Å)	13.855(3)	27.008(5)	18.792(4)	11.152(2)	7.0171(14)
α (deg)	103.63(3)	90	90	90	90
β (deg)	100.11(3)	90.21(3)	111.23(3)	90	93.52(3)
γ (deg)	105.71(3)	90	90	90	90
V (Å ³)	1339.0(5)	2077.5(7)	6314(2)	8108(3)	726.2(3)
Z	2	4	8	16	4
absorp coeff (cm ⁻¹)	35.59	34.49	12.63	10.04	1.06
no. of reflns collected	11 084	12 764	13 127	5196	1500
no. of indep reflns	6550 [R(int) = 0.0304]	4493 [R(int) = 0.0516]	7817 [R(int) = 0.0446]	5196 [R(int) = 0.0000]	953 [R(int) = 0.0323]
T _{max} /T _{min}	0.7173/0.5363	0.7699/0.5455	0.8841/0.8841	0.9063/0.8244	0.9916/0.9792
GOF	1.014	1.023	1.009	1.031	1.057
final R indices [I > 2 σ (I)]	R ₁ = 0.0311, wR ₂ = 0.0715	R ₁ = 0.0440, wR ₂ = 0.1064	R ₁ = 0.0421, wR ₂ = 0.0775	R ₁ = 0.0409, wR ₂ = 0.0914	R ₁ = 0.0558, wR ₂ = 0.1534
R indices (all data)	R ₁ = 0.0438, wR ₂ = 0.0758	R ₁ = 0.0604, wR ₂ = 0.1187	R ₁ = 0.0904, wR ₂ = 0.0880	R ₁ = 0.0573, wR ₂ = 0.0984	R ₁ = 0.0802, wR ₂ = 0.1677
largest diff peak and hole (e Å ⁻³)	0.578 and -0.943	1.073 and -1.185	0.582 and -0.879	0.374 and -0.613	0.400 and -0.406

least-squares refinement (least-squares function minimized: $\sum w(F_o^2 - F_c^2)^2$) on F were applied until convergence of unweighted and weighted factors of $R = \sum ||F_o| - |F_c|| / \sum |F_o|$; $R_w = \{ \sum [w(F_o^2 - F_c^2)^2] / \sum [w(F_o^2)] \}^{1/2}$. Crystal data and experimental details for the crystals of **9**, **11**, **12**, **13**, and **14** are given in Table 3.

Computational Details. The calculations were performed with the Gaussian03 package³⁰ at the B3PW91 level.³¹ Molybdenum was represented by the relativistic effective core potential (RECP) from the Stuttgart group and the associated basis set (SDDALL

keyword in Gaussian03),³² augmented by an f polarization function ($\alpha = 1.043$).³³ Phosphorus was represented by the relativistic effective core potential (RECP) from the Stuttgart group and the associated basis set (SDDALL keyword in Gaussian03),³⁴ augmented by a d polarization function ($\alpha = 0.387$).³⁵ A 6-31G(d,p) basis set was used for all the other atoms (C, N, H, O).³⁶ The geometry optimizations for (L-L)Mo(CO)₄ or *cis*-(L)₂Mo(CO)₄ were performed without any symmetry constraint followed by analytical frequency calculations to confirm that a minimum had been reached.

Acknowledgment. Generous financial support by the U.S. Department of Energy and the Spanish Ministerio de Educacion y Ciencia (fellowship to M.P. and funding to E.P. within the Programa de Movilidad de Profesor Universitarios) is gratefully acknowledged.

Supporting Information Available: Tables of crystallographic data, atomic coordinates, bond lengths, and bond angles for complexes **9**, **11**, **12**, **13**, and **14**. This material is available free of charge via the Internet at <http://pubs.acs.org>.

OM800021C

(30) Frisch, M. J.; Trucks, G. W.; Schlegel, H. B.; Scuseria, G. E.; Robb, M. A.; Cheeseman, J. R.; Montgomery, J. A., Jr.; Vreven, T.; Kudin, K. N.; Burant, J. C.; Millam, J. M.; Iyengar, S. S.; Tomasi, J.; Barone, V.; Mennucci, B.; Cossi, M.; Scalmani, G.; Rega, N.; Petersson, G. A.; Nakatsuji, H.; Hada, M.; Ehara, M.; Toyota, K.; Fukuda, R.; Hasegawa, J.; Ishida, M.; Nakajima, T.; Honda, Y.; Kitao, O.; Nakai, H.; Klene, M.; Li, X.; Knox, J. E.; Hratchian, H. P.; Cross, J. B.; Bakken, V.; Adamo, C.; Jaramillo, J.; Gomperts, R.; Stratmann, R. E.; Yazyev, O.; Austin, A. J.; Cammi, R.; Pomelli, C.; Ochterski, J. W.; Ayala, P. Y.; Morokuma, K.; Voth, G. A.; Salvador, P.; Dannenberg, J. J.; Zakrzewski, V. G.; Dapprich, S.; Daniels, A. D.; Strain, M. C.; Farkas, O.; Malick, D. K.; Rabuck, A. D.; Raghavachari, K.; Foresman, J. B.; Ortiz, J. V.; Cui, Q.; Baboul, A. G.; Clifford, S.; Cioslowski, J.; Stefanov, B. B.; Liu, G.; Liashenko, A.; Piskorz, P.; Komaromi, I.; Martin, R. L.; Fox, D. J.; Keith, T.; Al-Laham, M. A.; Peng, C. Y.; Nanayakkara, A.; Challacombe, M.; Gill, P. M. W.; Johnson, B.; Chen, W.; Wong, M. W.; Gonzalez, C.; Pople, J. A. *Gaussian 03, Revision C.02*; Gaussian, Inc.: Wallingford, CT, 2004.

(31) (a) Becke, A. D. *J. Chem. Phys.* **1993**, *98*, 5648. (b) Perdew, J. P.; Wang, W. *Phys. Rev. B* **1992**, *45*, 13244.

(32) Andrae, D.; Haussermann, U.; Dolg, M.; Stoll, H.; Preuss, H. *Theor. Chim. Acta* **1990**, *77*, 123.

(33) Ehlers, A. W.; Bohme, M.; Dapprich, S.; Gobbi, A.; Hollwarth, A.; Jonas, V.; Kohler, K. F.; Stegmann, R.; Veldkamp, A.; Frenking, G. *Chem. Phys. Lett.* **1993**, *208*, 111.

(34) Bergner, A.; Dolg, M.; Kuchle, W.; Stoll, H.; Preuss, H. *Mol. Phys.* **1993**, *80*, 1431.

(35) Hollwarth, A.; Bohme, M.; Dapprich, S.; Ehlers, A. W.; Gobbi, A.; Jonas, V.; Kohler, K. F.; Stegmann, R.; Veldkamp, A.; Frenking, G. *Chem. Phys. Lett.* **1993**, *208*, 237.

(36) Hariharan, P. C.; Pople, J. A. *Theor. Chim. Acta* **1973**, *28*, 213.